Accepted Manuscript

Direct Recoil Spectroscopy of adsorbed Atoms and Self-Assembled Monolayers on Cu(001)

L. Salazar Alarcón, J. Jia, A. Carrera, V.A. Esaulov, H. Ascolani, J.E. Gayone, E.A. Sánchez, O. Grizzi

PII: S0042-207X(14)00026-8

DOI: 10.1016/j.vacuum.2014.01.017

Reference: VAC 6214

To appear in: *Vacuum*

Received Date: 1 October 2013

Revised Date: 9 January 2014

Accepted Date: 10 January 2014

Please cite this article as: Alarcón LS, Jia J, Carrera A, Esaulov VA, H. Ascolani , Gayone JE, Sánchez EA, Grizzi O, Direct Recoil Spectroscopy of adsorbed Atoms and Self-Assembled Monolayers on Cu(001), *Vaccum* (2014), doi: 10.1016/j.vacuum.2014.01.017.

Direct Recoil Spectroscopy of adsorbed Atoms and Self-Assembled Monolayers on Cu(001)

L. Salazar Alarcón,*J. Jia[#], A. Carrera*, V.A. Esaulov,[#] H. Ascolani*, J.E. Gayone*, E.A. Sánchez* and O. Grizzi*

** Centro Atómico Bariloche-CNEA, Instituto Balseiro-UNC, CONICET, 8400 S.C. de Bariloche, Río Negro, Argentina*
[#] CNRS, Institut des Sciences Moléculaires d'Orsay, UMR 8412, Université-Paris Sud and CNRS, Bâtiment 351, 91405 Orsay, France.

Abstract: We present results of adsorption experiments of Sn and 1,4-benzenedimethanethiol (BDMT) on Cu(001), which illustrate the capabilities of a new setup specifically designed to perform surface studies by Direct Recoil Spectroscopy (DRS). The system consists of three UHV chambers connected in series with a 1-100 keV ion accelerator. In the main UHV chamber the DRS technique is combined with other more standard techniques such as Auger and Energy Loss Electron Spectroscopy, and Low Energy Electron Diffraction. The capabilities of the instrument are exemplified by two adsorption studies on the (001) face of Cu. First we describe measurements for 0.5 monolayer of Sn adsorbed on Cu that are in agreement with the crystallographic symmetry $(3\sqrt{2}x\sqrt{2})$R45^o seen by LEED and the appearance of Cu vacancies along the [100] direction. Then we present a study of self-assembling of 1,4-benzenedimethanethiol (BDMT) on Cu(001) from the vapour phase. For this system we show that it is possible to form a standing-up phase at large exposures, of the order of 10^6 L, and discuss its stability with temperature. We also discuss a S enrichment effect induced during the first adsorption stages of BDMT.

Keywords: Direct Recoil Spectroscopy, Dithiols, BDMT Self-assembled Monolayers, Sn/Cu Surface Alloy

1-Introduction

Direct Recoil Spectroscopy (DRS) is a variation of the better known Ion Scattering Spectroscopy [1-4] in which the observation is set at forward angles with the aim of detecting primary recoiled particles (adsorbed and substrate atoms) together with the scattered projectiles. In contrast with the backscattering geometry, here most of the information about the surface comes from the analysis of the intensity of recoiled particles.With the exception of some specific cases the ion fractions in recoils are very small, making the Time of Flight (TOF) method the preferred one for spectroscopy. As it has been described before [5], among the advantages of DRS are its capability to detect H and light adsorbed atoms, the very high top layer sensitivity, a higher cross-section and fast acquisition times, which in turn results in very low damage of the analyzed surface. In comparison to the backscattering geometry DRS has a lower mass resolution and a higher contribution from multiple scattering collisions. The advantages enumerated above have made of TOF-DRS an interesting technique to study adsorption phenomena, for atoms and in particular for organic molecules adsorbed at surfaces [6]. In this report we describe the instrument developed at the Surface Science Group in Bariloche which combines both back (ion scattering) and forward (direct recoil) spectroscopies with other techniques including Micro Channel Plate - Low Energy Electron Diffraction (MCP-LEED), Ultraviolet Photoelectron Spectroscopy (UPS), Auger (AES) and High Resolution Energy Loss Spectroscopy (EELS). In order to show the capabilities of the instrument, in this report we apply TOF-DRS to two different problems of present interest: 1) the crystallography of the surface alloy formed during adsorption of 0.5 monolayer of Sn on Cu(001), and 2) the formation of a self-assembled monolayer (SAM) of 1,4-benzenedimethanethiol (BDMT) on Cu(001) from the vapour phase and its thermal stability. The paper is organized as follows, in the next section we describe the main characteristics of the experimental set up and its design criteria, then, in section 3, we present the Sn/Cu(001) measurements, including the motivation for this study, the measurements and specific conclusions. In section 4 we present the BDMT/Cu(001) study and finally in section 5 we present general conclusions.

2- Experimental details

In TOF-DRS a pulsed ion beam at keV energies hits the surface and recoils and projectiles emitted at forward angles are analyzed with TOF techniques. The typical characteristics of the pulsed beam are 10-50 kHz and 10-50 nsec pulse width. The simple

equations governing the scattering processes as well as details for the cross-section variation with mass and observation angle, together with the effects of the crystal structure, have been discussed in detail in many references, see for example [7]. In order to impart sufficient energy to recoils which are mostly neutrals, so that they can be detected efficiently with channeltrons or channelplates, it is convenient to work with projectile energies in the range of some keVs. For DRS the observation angle has to be selected in such a way that the more intense projectile peak (scattering peak) appears separated in the TOF scale from the desired recoiled peaks, which usually are narrower and considerably less intense. This characteristic implies that the best observation angle depends on the system to be studied. To overcome this limitation, systems with continuously rotating TOF spectrometers have been designed [8, 9] where the continuous variation of the observation angle allows measurements at both the forward and the backward scattering geometry. A problem associated with these big systems is the large chamber space used by the technique which leaves little room for other techniques of surface analysis. Another interesting feature of the TOF-DRS detection method is its capability of working at pressures that would be too high for other techniques; this aspect of DRS was used before [10] to follow the growth of films during high exposures at real times.

The Bariloche system was designed with the major points discussed above in mind. The system comprises three UHV chambers connected in series with a radio frequency ion source working from 1 to 100 keV, as schematized in figure 1. The beam is mass analyzed with a switching magnet before entering chamber 1, and can be collimated with variable apertures and pulsed at different points of the line. The small chamber closest to the beam source (chamber 1) is mainly used for studies of radiation damage. The second chamber (middle) has facilities for sample preparation by ion sputtering and annealing with both the main beam line or with a secondary ion gun. The manipulator allows rotations around both the polar and azimuthal angle of incidence, and cooling of the sample. This chamber has two ~1 meter long TOF drift tubes located at fixed angles of 45^{o} and 135^{o}. The main use of this chamber is to study organic molecule adsorption phenomena requiring very large exposure regimes, typically of the order of Mega Langmuirs, which would be not easily compatible with other surface analysis methods.

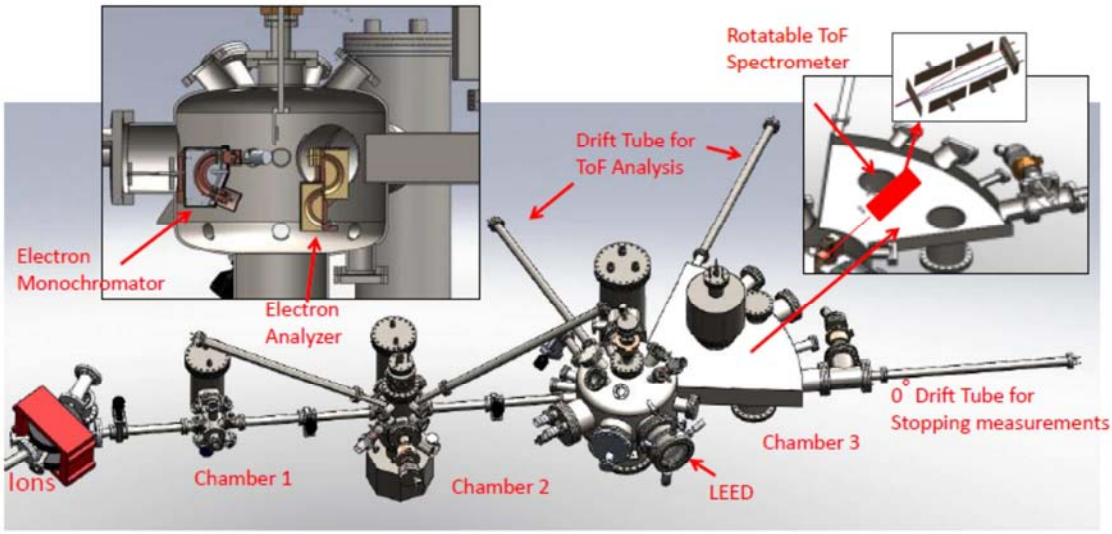

Figure 1: Sketch of the Bariloche setup for TOF-ISS, TOF-DRS, LEED, UPS, AES and HREELS.

The main analysis chamber (chamber 3, figure 1) has a big wing housing a rotatable TOF spectrometer that moves only within the most useful range of forward observation angles: 0 to 65^{o}. This wing is welded onto a relatively large mu metal chamber (45 cm in diameter) allowing the mounting of other standard techniques (HEELS, AES, UPS, LEED). The rotatable TOF spectrometer has collimation apertures, deflecting plates and three anodes that in conjunction allow performing measurements of ion fractions in the scattered or recoiled beam geometry. Other fixed ports located at forward (0. 30, 45, 65^{o}) or backward (118^{o}) angles complete the TOF arrangement. In particular, the 0^{o} TOF port has been used for measurements of stopping powers in thin foils by the transmission method [11].

The main chamber is prepared for studies of atom and organic molecule adsorption, in this sense, the LEED optics has channelplate amplification which requires a lower electron dose to obtain a pattern, thus reducing the damage of the molecular layer. A 35 mm full hemispherical electron analyzer is mounted on an independent rotatable platform and is used for UPS and also, in conjunction with the electron monochromator, allows studies of HREELS.

Several types of evaporators can be mounted depending on the necessity. In the present measurements we used for Sn a carefully degassed Knudsen cell, working at pressures lower than 4x10^{-9} mBar. For the self-assembly study we used pure (98%) BDMT powder from Sigma Aldrich, which was introduced in a glass tube connected to the chamber through a leak valve. A 4 mm diameter tube running from the leak valve to about 2 cm from the sample was used to direct the BDMT flux towards the sample. The BDMT container, leak valve and tube were maintained around 80^{o}C during evaporations.

3- Experimental Results and discussion

3.1 Characterization of the $(3\sqrt{2}x\sqrt{2})$ R45° Sn/Cu(001) surface

Surface alloys have attracted much interest over the years due, especially, to their adaptable electronic, magnetic and catalytic properties [12]. Commonly, the deposition of 0.5 monolayer of metal atoms on (001) surfaces of noble metals produces single layer surface alloys with a 50%/50% composition and a $(\sqrt{2}x\sqrt{2})$ $R45^{o}$ periodicity. An exception to this trend is the Sn/Cu(001) system which at room temperature (RT) forms a single-layer surface alloy with $Sn_{0.5}Cu_{0.3}$ composition and $(3\sqrt{2}x\sqrt{2})R45^{o}$ periodicity [13]. Recently, this system was found to exhibit a remarkably interesting behavior with temperature [14 - 15]. Figure 2 shows a LEED pattern of this phase, where the two 90°-rotated domains coexist. This structure is obtained when a coverage of 0.5 monolayer of Sn is deposited on the Cu surface at room temperature. The accepted model for this phase, together with the Cu(001) surface is schematically shown in figure 3(a). The Sn atoms replace Cu surface atoms forming a single layer surface alloy. In addition there is a vacancy line of Cu atoms along the [100] direction, causing 2 lines of Sn atoms out of three to be 0.1 Å lower, resulting in the $(3\sqrt{2}x\sqrt{2})$ periodicity [13, 15, 16, 17]. This reconstruction undergoes a reversible order-disorder transition to a $(\sqrt{2}x\sqrt{2})$R45° phase when the temperature increases above 360 K, which is related to the disordering of the Cu vacancies. TOF-DRS and ISS are particularly suitable to monitor the formation of vacancies [5, 18]; in a previous work we applied the TOF-DRS facility to study the Cu vacancy evolution across the phase transition [15]. More recently, a medium energy ion scattering spectroscopy (MEIS) study has confirmed the model of Cu-vacancy lines [19]. In this section we use TOF-DRS to analyze the (3√2 x√2) R45° Sn/Cu(001) reconstruction. In particular, we exploit the strong surface sensitivity of the technique to obtain qualitative information of the top surface alloy.

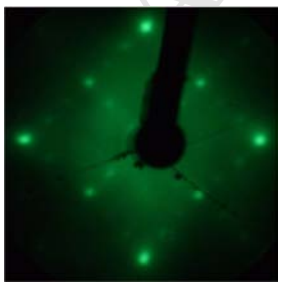

Figure 2: LEED pattern for the $\left(3\sqrt{2}x\sqrt{2}\right)$ *R45° Sn/Cu(001) surface alloy*

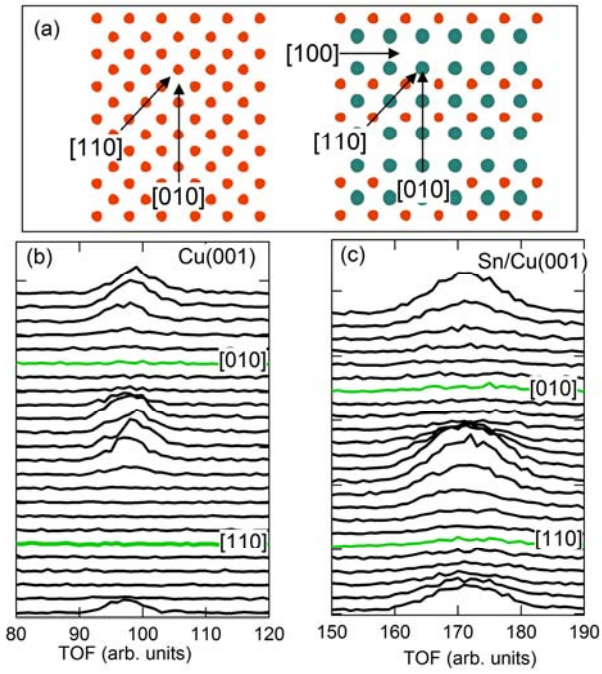

Figure 3: (a) Schematics of the clean (left) and the 0.5 monolayer Sn/Cu(001) surface (right). Red (blue) circles correspond to Cu (Sn) atoms. (b) TOF-DRS spectra as a function of the azimuthal angle in the region of the Cu recoil peak for the pure substrate, and (c) spectra in the region of the Sn recoil peak for the Sn/Cu(001). The spectra were obtained at a fixed incident polar angle of 15° with respect to the surface plane.

The Cu(001) substrate was prepared by grazing Ar sputtering at 20 keV, 2-3° incidence with respect to the surface plane and annealing to 720 K. During sputtering the sample was kept under continuous rotation around its normal, in order to change the azimuthal incidence angle. This procedure was very effective to smooth out the initial surface roughness. The DRS spectra were acquired with a 5 keV $^{20}Ne^{+}$ ion-pulsed beam and a scattering angle of 30°. Figure 3(b) shows a set of TOF-DRS spectra as a function of the azimuthal angle for a fixed incident angle of 15^{o} measured from the surface plane. At certain azimuthal directions a peak is observed which corresponds to the Cu recoil atoms emitted in collisions with the primary incident beam. Although a full trajectory simulation is needed to reproduce the dependence with azimuth of all the features observed in the TOF spectra, direct information regarding some aspects of the structure can be obtained by plotting the area of the peak as a function of azimuth as is done in Figure 4 (red curve). This intensity presents strong variations with azimuth which reflects the symmetry of the top atomic layer. Indeed, along the [010] and [110] directions there are strong minima which can be rationalized in terms of shadowing of the ion-beam incoming-trajectories or blocking of the emitted-recoil outgoing-trajectories. Along the compact azimuthal direction the distance between two consecutive Cu surface atoms is small and the shadowing and blocking effects are strong resulting in a major

attenuation of the Cu recoil peak. The [110] direction is the most compact one, resulting in a wider and deeper minimum. On the other hand, when the azimuthal angle is moved away from this compact directions, Cu surface atoms are moved away from the shadow and blocking regions, and the intensity increases. As a general rule, at rather small incident angles, the deeper minima in azimuthal scans are associated with compact directions.

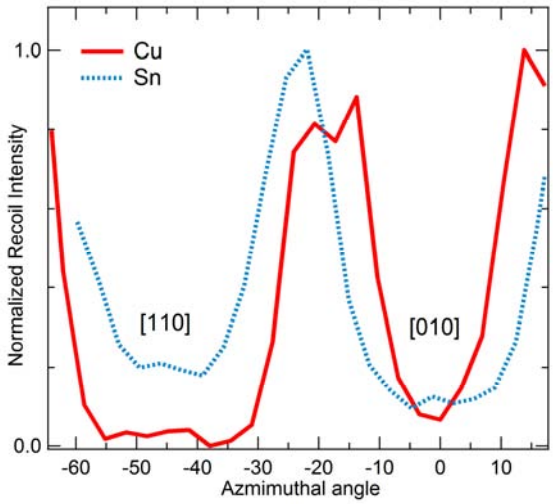

Figure 4: Variation of the Cu recoil intensity (red, solid) and Sn intensity (blue, dashed) versus azimuth for pure Cu(001) and for Sn/Cu(001).

Figure 3(c) shows the set of TOF spectra measured at the same incidence and azimuthal angles as in figure 3(b) for the Sn/Cu surface. In this case, the TOF scale region corresponds to the Sn recoils. Similarly to the Cu surface discussed above, the Sn recoil intensity shows strong variations of the peak intensity with azimuth (figure 4, blue dotted line). This curve presents two pronounced minima at [010] and [110], however, in this case the deeper and wider minima correspond to the [010] direction indicating that this is the most compact one. This is consistent with the model discussed above, where the Sn atoms are arranged in a lattice rotated 45 degrees with respect to the clean Cu lattice. However, along the [110] direction there is a Cu atom between 2 consecutive Sn atoms. The fact that the deeper minimum is observed along the [010] direction shows that the Cu atoms are located below the Sn ones. Experimental and theoretical results report values of ~0.4 A for the Sn-Cu vertical distance [13, 17, 19].

As discussed above, the shadowing and blocking effects are mainly governed by the distance between two consecutive atoms, being more important when this distance is small. This property is particularly suitable to study and detect vacancy lines in surfaces. In order to explore it in the $(3\sqrt{2}x\sqrt{2})$ structure, we fixed the azimuthal angle along the [010] direction

and measured DRS spectra at different incident polar angles. In Figure 5 we show the intensity of the Cu recoil versus incidence angle for the clean Cu surface and the $\left(3\sqrt{2}x\sqrt{2}\right)$ phase. Although we are adsorbing a rather heavy atom, the intensity of the Cu recoils increases in the whole range of measured angles. In the inset of the figure 4, we show the spectra for 20^{o} (see arrow), where for the clean surface no peak is observed, but after forming the surface alloy a clear Cu recoil peak appears. This increase is explained by the appearance of Cu vacancies. When a vacancy is formed along the [100] direction, the distance between 2 consecutive Cu atoms along the perpendicular direction [010] increases by a factor of two. Therefore, the shadowing and blocking effects become less important causing the increase of the Cu recoil intensity, resulting in a direct evidence of the existence of the vacancy lines.

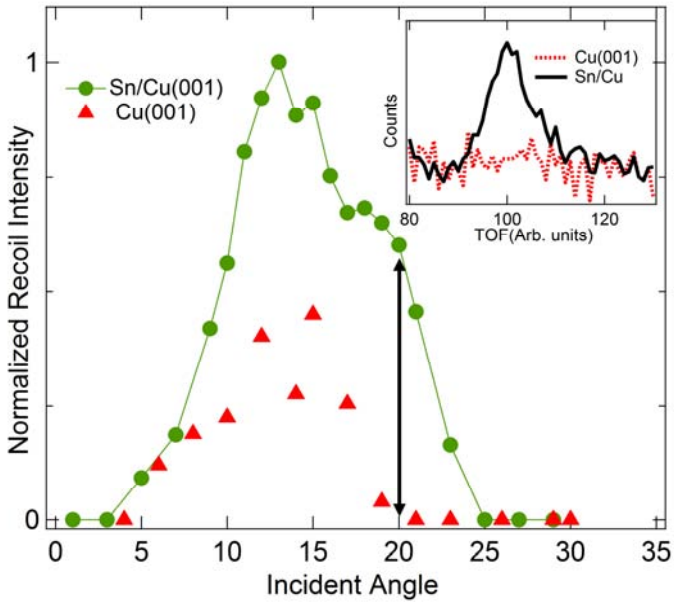

Figure 5: Variation of the Cu recoil peak area with incidence angle along the [010] direction for the pure substrate and for Sn/Cu. The Cu intensity observed for the pure substrate (from green spectrum along this direction on figure 3(b)) is attributed to initial defects. Inset: corresponding spectra measured at 20^{o} incidence.

3.2 Self-assembling of 1,4-benzenedimethanethiol on the Cu(001) surface

In this section we present another example where we use TOF-DRS for characterizing a different type of adsorbate, an organic molecule (BDMT) on the same substrate (Cu(001)) and the thermal stability of this system. Besides the possibility of detecting hydrogen atoms on the surface, there are two other aspects of the technique that are particularly important here: 1) it

generates very little damage on the films due to the low fluence required to get a spectrum, and 2) it can be very sensitive to detect which of the molecule atoms are exposed at the vacuum interface.

The major part of the studies of dithiol adsorption has been carried out earlier on Au surfaces since this substrate has good inertness, high affinity of S for Au, and different high quality SAMs can be prepared by dipping the sample in the appropriate solution [20]. For oxidizable surfaces a vacuum approach, where a clean surface is exposed to the vapours of the corresponding thiol or dithiol may be an interesting alternative [21-25] to the solution approach [26, 27]. Less inert surfaces usually require special surface treatment to prevent contamination with O, since this contamination can impair the SAM formation as is the case for Cu [28]. In particular, the interest in the interaction between Cu and different type of thiols and dithiols is related to the possibility of using it for surface protection [29, 30], or for depositing metallic nanoparticles [31].

In most examples of self-assembled dithiol monolayers prepared from the vapour approach it was shown that the molecules adopt first a configuration with both S atoms bonded to the substrate. Transition from this lying down configuration to the desirable one with standing-up molecules, i.e., having one thiol end exposed to the vacuum interface is sometimes possible at very high exposures, typically in the order of the Mega Langmuir [22, 24]. A question of great importance is when and under which experimental conditions this transition takes place [22 - 24, 32]. The order and the stability of these layers with the surface temperature are also important points for device fabrication.

Different techniques were used to characterize the molecule configuration, among them spectroscopic ellipsometry [26, 27, 33], XPS, NEXAFS [27], and IRRAS [26]. In the present work we use TOF-DRS to follow the growth of BDMT/Cu(001) *in situ*. We show that the layer sensitivity can be adjusted by the selection of the incident angle, that all the elements of the molecule can be detected with the appropriate projectile, and that some information about the molecule configuration can be provided.

Figure 6 shows several spectra taken at 20^{o} incidence with 4.2 keV Ar^{+} ions as a function of BDMT exposure. The most important features are the emergence of the C and H recoil peaks, the shift and broadening of the Ar scattering off substrate and the disappearance of the Cu recoil peak. The top spectrum, taken after an exposure of 10^{6} L, corresponds to saturation in the sense that further exposure produces no change in the spectra. We show below that this condition corresponds to a configuration with most molecules in the standing-

up orientation. The Cu recoil peak disappears at much lower exposures than that required for saturation, of the order 10^3 L, which indicates that at this condition the surface is already fully covered with BDMT (in the lying down configuration, as it will be shown below).

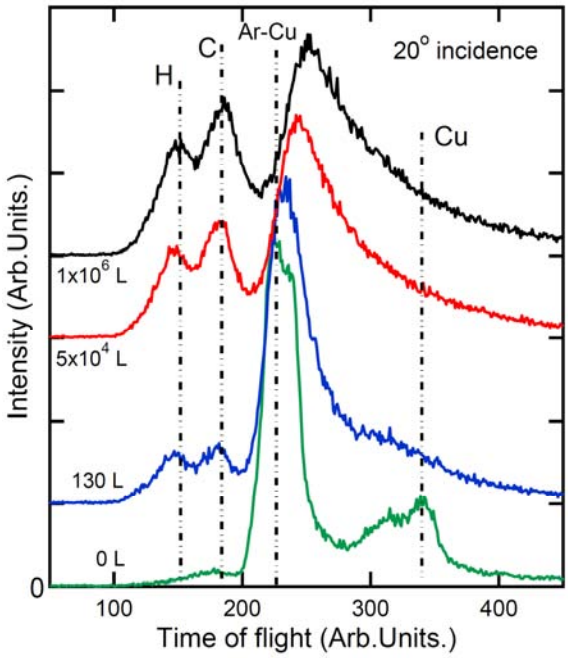

Figure 6: TOF-DRS spectra acquired for BDMT /Cu(001) at different BDMT exposures

At 20° incidence the Ar projectiles penetrate the BDMT layer and some multiple scattering from the substrate is possible at all coverages. TRIM simulations performed for the same molecule adsorbed on Au(111) suggested [22] that if the Ar – Cu multiple scattering peak can be seen under our present beam conditions the layer should not be thicker than one full monolayer (on the average), i.e., if there were a multilayer, the substrate contribution should disappear completely.

The top surface sensitivity can be enhanced at more grazing incident angles. Figure 7 shows two spectra taken at 5° for exposures of 390 L and 10^6 L (saturation). The bottom spectrum shows (besides the H and C peaks) only one broad structure that is mainly due to Ar multiple scattering. The lack of clear S associated peaks is an indication that most molecules are in a configuration where both S atoms are bonded to the surface and are therefore not accessible to the beam due to shadowing from the C ring. With increasing exposures (and BDMT pressure) the Ar multiple scattering structure is drastically reduced and the S associated peaks, i.e., the S recoil and the Ar scattering off S, can be clearly seen (top spectrum), which is an indication of the presence of S or thiol termination at the vacuum interface. In our geometry, the cross-section for Ar scattering off S and for S recoil production are similar, so both S associated peaks in the top spectrum come from S top layer

atoms, and not from Ar substrate collisions, as is the case at lower exposures. This suggests that most of the surface should be covered with a standing-up configuration. For the understanding of the collision process we draw in Figure 7 two molecule orientations that could generate the observed spectra, however these drawings should be considered only as qualitative.

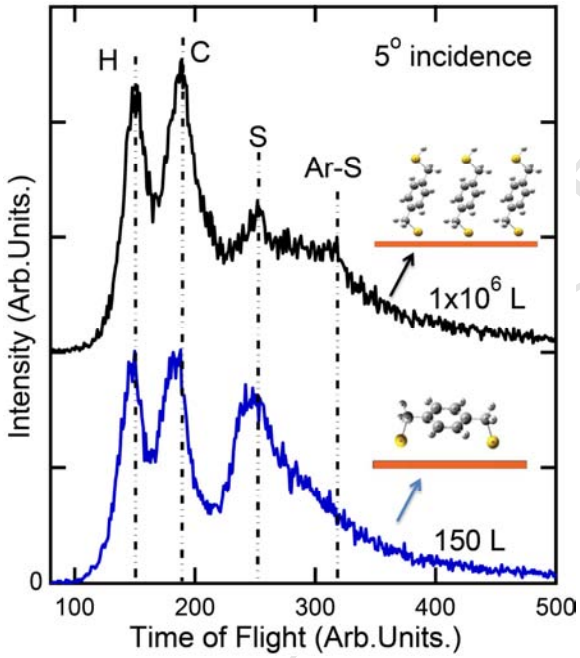

Figure 7: TOF-DRS spectra measured at grazing angles for the lying down phase (bottom) and at saturation, with thiols exposed to the vacuum interface (top). The two possible molecular arrangements are also indicated.

Integration of the different recoil peak areas (Figure 8) allows us to obtain a better understanding of the adsorption kinetics. At 20° incidence we observe the rapid attenuation of the substrate contribution, which is accompanied by the emergence of H and C recoil peaks. At these early exposures (some 10^3 L) the H and C intensities measured at grazing incidence (5°) saturate, indicating that the surface is completely covered. Up to this stage the adsorption proceeds very fast (note that the horizontal scale is logarithmic) and then more slowly, allowing some molecules to stand up beyond some 10^3 L. This change of orientation is visualized by the emergence of the S recoil peak at grazing angles. The process saturates around 10^6 L.

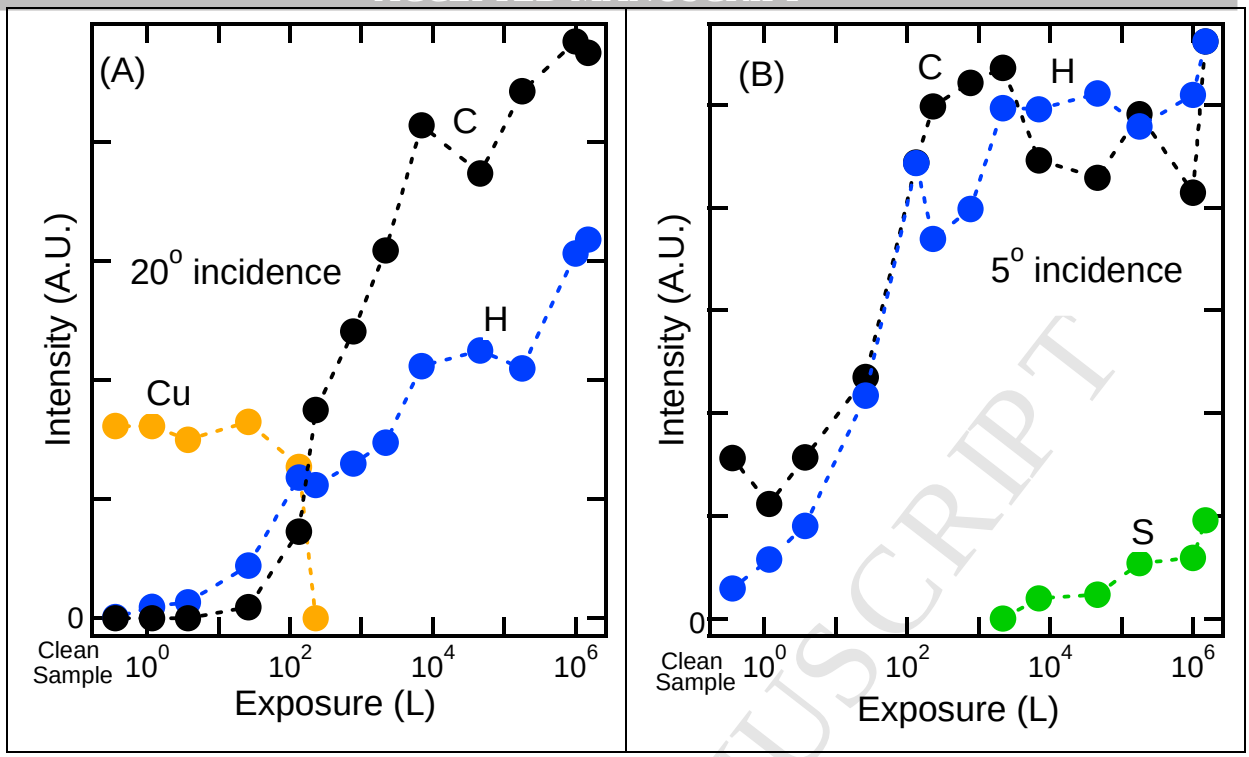

Figure 8: H, C, Cu and S TOF recoil peak areas measured with Ar ions at 20° (A) and at 5° (B) incidence as a function of BDMT exposure.

All the measurements shown in this work were carried out on the same Cu(001) single crystal. At the beginning of each measurement one verifies that the surface is free of contaminants such as O, H, C and particularly S, a condition that is obtained by cycles of sputtering and annealing. In spite of this careful treatment we detected a S signal during the initial steps of the BDMT adsorption. With Ar projectiles, the S peak appears at the right side of the Ar scattering peak and is difficult to observe particularly when the latter is very strong (at low coverages). The TOF position of S is also similar to that for a Cu surface recoil (Cu atoms going first to the surface and then to the detector). By using Kr ions, the S recoil peak appears at the left side of the scattering peak and is therefore more easily visible.

The series of spectra of figure 9 were acquired at 20° incidence with 3 keV Kr^+ ions as a function of BDMT exposure. Note that during the exposures, and where the C peak is still small, a narrow S recoil peak can be observed clearly. The S to C peak intensity ratio and its shape indicate that it is not coming from an intact BDMT molecule, one possibility is segregation due to some amount of S present in the Cu bulk. We have been working with Au and Ag samples for some years, using always the same procedures for surface treatments and purification of BDMT and never observed this effect on those substrates. This same sample did not show this effect when used with Sn and other molecules. Looking at the spectra for

increasing exposure we note that the strongest S recoil peak is observed before covering the surface completely. Upon increasing exposures the characteristic C/S recoil ratio for BDMT is attained, these recoil peaks increase further and become broader at very large exposures when the molecules stands up. With Kr ions, the H recoil peak is only detected as a small shoulder because of the low efficiency of the channeltron for low energy H atoms.

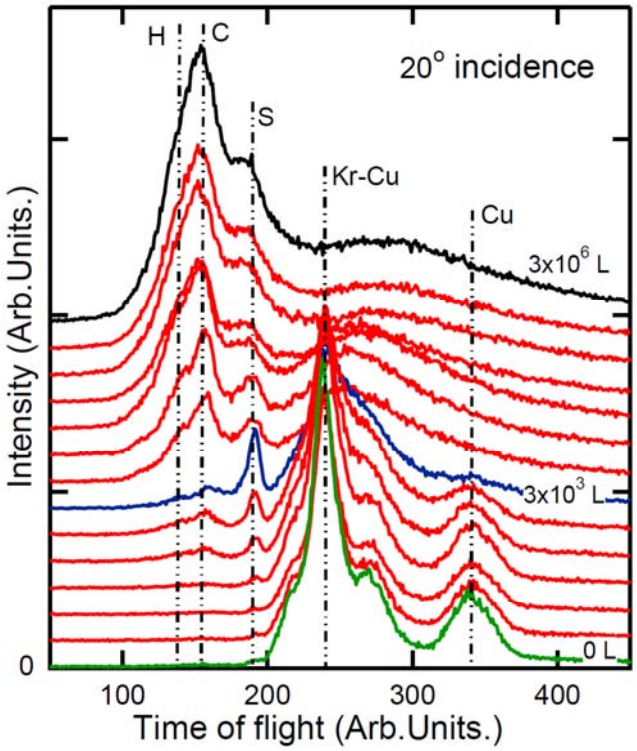

Figure 9: TOF- DRS spectra acquired with 3 keV Kr ions at 20° incidence versus BDMT exposure.

An alternative to the segregation effect might also be an initial strong reaction of Cu with the thiol leading to the appearance of an initial Cu sulphide dilute layer as this is known to happen in the Pd-thiol case [34]. This reaction should be accompanied by the partial desorption of the benzene product to explain the initial low C/S ratio. At present we do not have sufficient complementary data by other techniques to discern between these possibilities.

BDMT stability with sample temperature:

In order to study the stability of the BDMT layer we show in figures 10 (a-c) TOF-DRS spectra acquired with Ar and Kr ions at different sample temperatures. The most meaningful recoil peak areas are shown in figures 11 (a) and (b). For each run the spectra were acquired alternatively at 5° and at 20° after an exposure of ~3 10^6 L, corresponding to formation of the standing-up phase. The series of spectra measured with Ar and with Kr ions correspond to two different adsorption experiments carried out under the same conditions. The temperature

ramp is approximately 5 K/min which allows taking sufficient spectra for describing the layer behavior. The spectra at 20^o are more representative of the layer elemental composition while those at 5^o tell us about the fate of S at the top.

From RT up to 400 K there is a continuous and shallow decrease of all the molecule elements (H, C and S) suggesting that some (whole molecule) desorption is taking place. We have observed a similar trend for other thiols in Au. In the region around 370 K there is a reordering (or disordering) of the layer and the S features observed at 5^o, that are associated to having thiols exposed at the vacuum interface, disappear (two characteristic spectra are shown in Figure 10 (b)). These changes are accompanied by the emergence of the Ar multiple scattering off substrate (at 5^o) and a corresponding increase at 20^o, indicating that the remaining layer is getting thinner as it should correspond to a lying down layer. The surface is still fully covered since no Cu recoil is detected at 20^o. Then, around 400 – 450 K a strong reduction of the C and H recoil peak areas takes place (for spectra at 20^o) while the S peak tends to increase. The ratio of H/C peak areas is maintained constant during this range of temperatures, thus suggesting S-C bond breaking accompanied by desorption of the hydrocarbon molecular products. The S tends to remain at the surface even after annealing to 500 K. At the higher temperatures, above 500 K, there is a change in the H to C ratio, H tends to desorb completely while a small amount of C remains at the surface.

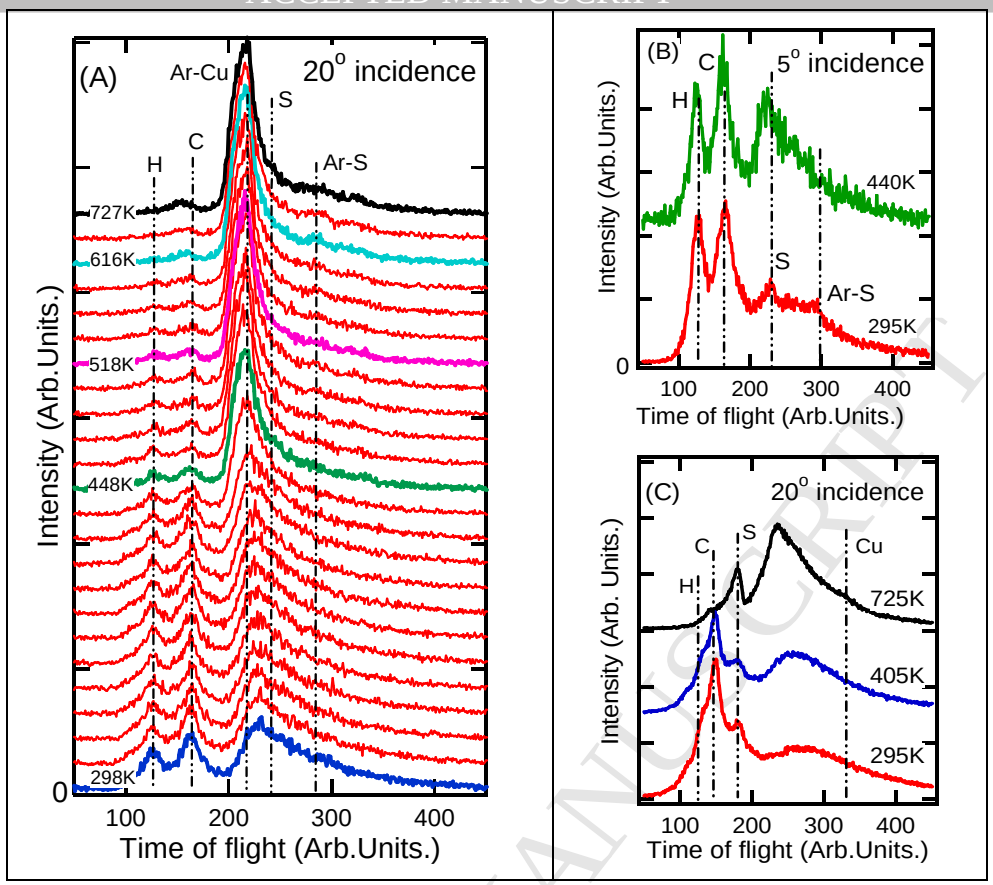

Figure 10: series of TOF- DRS spectra acquired at different sample temperatures with 4.2 keV Ar^+ ions at 20^o (A) and at 5^o (B), and with 3 keV Kr^+ ions at 20^o incidence (C).

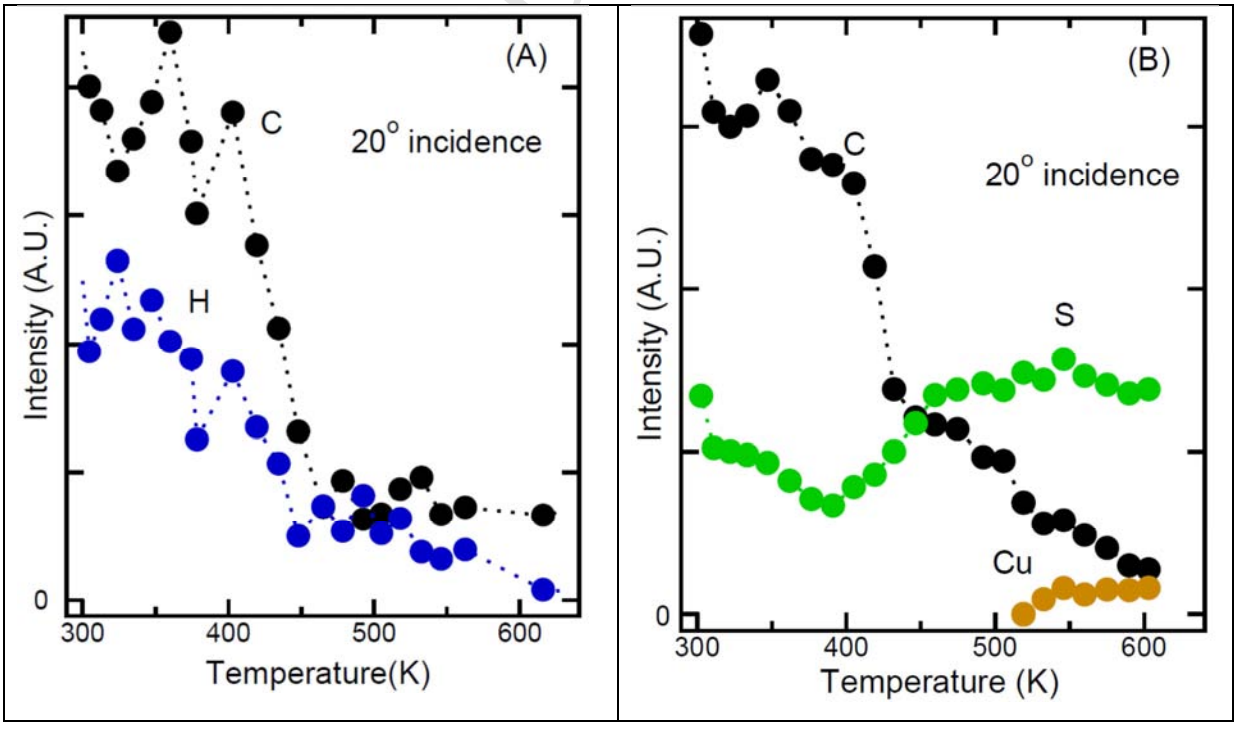

Figure 11: C, H, S and Cu Recoil peak areas measured with 4.2 keV Ar ions (a) and with 3.0 keV Kr ions (b) as a function of surface temperature.

General Conclusions:

We described a system designed for TOF-DRS and applied it to two different adsorption problems on the Cu(001) surface. First we extended a previous study of the $(3\sqrt{2}x\sqrt{2})$ R45^{o}Sn/Cu surface alloy showing that the azimuthal dependence of the Sn recoil peak area is consistent with a model where the Sn atoms are arranged in a lattice rotated 45 degrees with respect to the clean Cu lattice. The Cu recoil peak area measured along the [010] direction increases when 0.5 monolayer of Sn is adsorbed in correspondence with the generation of Cu vacancies. Then we presented TOF-DRS measurements of adsorption of 1,4-benzenedimethanethiol on the same substrate. We showed that at exposures of the order of the 10^3 L the surface becomes fully covered with BDMT molecules in a lying down configuration and upon higher exposures it is possible to incorporate more BDMT in a standing up configuration, i.e., having a thiol termination in the vacuum interface. For the first adsorption steps we detected S in larger amounts than would correspond to the adsorbed BDMT molecule. We suggested two possibilities for this effect: S segregation from the bulk or a sulphide layer formed initially which should be accompanied by desorption of the benzene products. A study of the BDMT layer versus temperature showed that there is a shallow desorption of the molecules starting close to RT and that the thiol termination is fully removed in the region 370-400 K. At this temperature the molecules are mostly in a lying-down configuration. Further annealing results in a surface covered with S and some C.

Acknowledgements: We acknowledge support from the French-Argentinean MinCyT-CNRS cooperation program (LIFAN), from Instituto de Nanociencia y Nanotecnología - CNEA, Universidad Nacional de Cuyo (06/C390 y 06/C383) and CONICET (PIP 112-200801-00958, 112-201101-00594).

References:

1. D.P. Woodruff and T.A. Delchar, Modern Techniques of Surface Science, Cambridge, Solid State Science Series, University Press, 1994.
2. Th. Fauster, Vacuum 38 (1988) 129.
3. H. Niehus, W. Heiland, E. Taglauer, Surf. Sci. Repts. 17 (1993) 213.
4. H.H. Brongersma, G.C. van Leerdam, Fundamental aspects of heterogeneous catalysis studied by particle beams, in: H.H. Brongersma, R.A. van Santen (Eds.), NATO ASI series B 265, 1991, p. 283.
5. J. Wayne Rabalais, Principles and Applications of Ion Scattering Spectrometry, Wiley Interscience, 2003.
6. L. M. Rodríguez, J.E. Gayone, E.A. Sánchez, H. Ascolani, O. Grizzi, M. Sánchez, B. Blum, G. Benitez, R.C. Salvarezza, Surf. Sci. 600 (2006) 2305
7. E.S. Parilis, L.M. Kishinevsky, N. Yu. Turaev, B.E. Baklitzky, F.F. Umarov, V. Kh. Verleger, S. L. Nizhnaya, and I.S. Bitensky, Atomic Collisions in Solid Surfaces, North Holland, 1993.
8. O. Grizzi, M. Shi, H. Bu, and J.W. Rabalais. Rev. Sci. Instr. 61 (2) (1990) 740.
9. C. Benazeth, P. Benoit-Cattin, P. Cafarelli, P. Reynes, J.P. Ziesel, N. Benazeth, NIM B 94 (4) (1994) 581.

10. V.S. Smentkowskiv, A. R. Krauss, O. Auciello, J. Im, D.M. Gruen, J. Holecek, K. Waters and J. A. Schultz, In Situ, Real-Time Studies of Film Growth Processes Using Ion Scattering and Direct Recoil Spectroscopy Techniques. MRS Proceedings, 1999, page 569.
11. L.N. SerkovicLoli, E.A. Sánchez, O. Grizzi, J.C. Eckardt, G.H. Lantschner and N.R. Arista. Phys. Rev. A. 81 (2) (2010) 022902 .
12. D. P. Woodruff, Surface Alloys and Alloy Surfaces, Elsevier Science, August 2002, ISBN: 9780444511522, 552 pages.
13. J. D. Fuhr, J. E. Gayone, J. Martínez-Blanco, E.G. García Michel, H. Ascolani, Phys. Rev. B 80 (2009) 115410.
14. J. Martínez-Blanco, V. Joco, H. Ascolani, A. Tejeda, C. Quirós, G. Panaccione, T. Balasubramanian, P. Segovia, and E. G. Michel1, Phys. Rev. B 72 (2005) 41401(R).
15. J. E. Gayone, A. Carrera, O. Grizzi, S. Bengió, E. A. Sánchez, J. Martínez-Blanco, E. G. Michel, J. D. Fuhr, and H. Ascolani. Phys. Rev. B 82 (2010) 035420.
16. J. Martínez-Blanco, V. Joco, C. Quirós, P. Segovia, E.G. Michel, J. Phys. Condens. Matter 21 (2009) 134011
17. K. Pussi, E. Al Shamaileh, E. McLoughin, A. A. Cafolla, and M. Lindroos, Surf. Sci. 24 (2004) 549.
18. H. Niehus, Surf. Sci. 145 (2-3) (1984) 407.
19. Walker et al, Surf. Sci. 605 (2011) 1934-1940.
20. Hicham Hamoudi, Zhiang Guo, Mirko Prato, Celine Dablemont, Wan Quan Zheng,Bernard Bourguignon, Maurizio Canepa and Vladimir A. Esaulov. Phys. Chem. Chem. Phys. 2008, 10, 6836–6841.
21. L. Pasquali, F. Terzi, R. Seeber, B.P. Doyle, S. Nannarone, J. Chem. Phys. 128 (2008) 13471.
22. L. Salazar Alarcón, L. Chen, V. A. Esaulov, J.E. Gayone, E.A. Sánchez, O. Grizzi, J. Phys. Chem. C. 114 (2010) 19993.
23. L.J. Salazar Alarcón, L.J. Cristina, J. Shen, J. Jia, V. A. Esaulov, E.A. Sanchez, and O. Grizzi, J. Phys. Chem. C, 2013, DOI: 10.1021/jp403348s
24. J. Jia, S. Mukherjee, H. Hamoudi , S. Nannarone , L. Pasquali , and V. A. Esaulov, J. Phys. Chem. C 117 (9) (2013) 4625.
25. L. M. Rodríguez, J. E. Gayone, E. A. Sánchez, O. Grizzi, B. Blum, R. C. Salvarezza, L. Xi, and W. M. Lau. J. Am. Chem. Soc. 129 (25) (2007) 7807.
26. H. Hamoudi, M. Prato, C. Dablemont, O. Cavalleri, M. Canepa, V.A. Esaulov, Langmuir 26 (2010) 7242.
27. L. Pasquali, F. Terzi, R. Seeber, S. Nannarone, D. Datta, C. Dablemont, H. Hamoudi M. Canepa, V.A. Esaulov, Langmuir 27 (2008) 4713.
28. Cl. Amato, S. Devillers, P. Calas, J. Delhalle, Z. Mekhalif, Langmuir 24 (2008) 10879.
29. H. Ron, H. Cohen, S. Matlis, M. Rappaport, and I. Rubinstein, J. Phys. Chem. B 102 (1998) 9861.
30. K. Jennings, J. C. Munro, T. H. Yong, and P. E. Laibinis, *Langmuir* 14 (21) (1998) 6130.
31. D. Aldakov, Y. Bonnassieux, B. Geffroy, and S. Palacin, ACS Appl. Mater. Interfaces 1 (3) (2009) 584.
32. V. Chaudhari, M.N.K. Harish, S. Sampath, and V.A. Esaulov, J. Phys. Chem. C 115 (33) (2011) 16518.
33. M. Canepa, "*A Surface Scientist's View on Spectroscopic Ellipsometry*", Springer Series in Surface Sciences. Volume 51, 2013, Surface Science Techniques, Editors: GianangeloBracco, Bodil Holst ISBN: 978-3-642-34242-4.
34. J. C. Love, D. B. Wolfe, R. Haasch, M. L. Chabinyc, K. E. Paul, G. M. Whitesides, and R. G. Nuzzo, J. Am. Chem. Soc. 125 (2003) 2597-2609.

Figure captions:

Figure 1: Sketch of the Bariloche setup for TOF-ISS, TOF-DRS, LEED, UPS, AES and HREELS.

Figure 2: LEED pattern for the $\left(3\sqrt{\mathbf{2}}\mathbf{x}\sqrt{\mathbf{2}}\right)$ R45° Sn/Cu(001) surface alloy

Figure 3: (a) Schematics of the clean (left) and the 0.5 monolayer Sn/Cu(001) surface (right). Red (blue) circles correspond to Cu (Sn) atoms. (b) TOF-DRS spectra as a function of the azimuthal angle in the region of the Cu recoil peak for the pure substrate, and (c) spectra in the region of the Sn recoil peak for the Sn/Cu(001). The spectra were obtained at a fixed incident polar angle of 15° with respect to the surface plane.

Figure 4: Variation of the Cu recoil intensity (red, solid) and Sn intensity (blue, dashed) versus azimuth for pure Cu(001) and for Sn/Cu(001).

Figure 5: Variation of the Cu recoil peak area with incidence angle along the [010] direction for the pure substrate and for Sn/Cu. The Cu intensity observed for the pure substrate (from green spectrum along this direction on figure 3(b)) is attributed to initial defects. Inset: corresponding spectra measured at 20^o incidence.

Figure 6: TOF-DRS spectra acquired for BDMT /Cu(001) at different BDMT exposures

Figure 7: TOF-DRS spectra measured at grazing angles for the lying down phase (bottom) and at saturation, with thiols exposed to the vacuum interface (top). The two possible molecular arrangements are also indicated.

Figure 8: H, C, Cu and S TOF recoil peak areas measured with Ar ions at 20^o (A) and at 5^o (B) incidence as a function of BDMT exposure.

Figure 9: TOF- DRS spectra acquired with 3 keV Kr ions at 20^o incidence versus BDMT exposure.

Figure 10: series of TOF- DRS spectra acquired at different sample temperatures with 4.2 keV Ar^+ ions at 20^o (A) and at 5^o (B), and with 3 keV Kr^+ ions at 20^o incidence (C).

Figure 11: C, H, S and Cu Recoil peak areas measured with 4.2 keV Ar ions (a) and with 3.0 keV Kr ions (b) as a function of surface temperature.

- We describe a UHV equipment combining direct recoil spectroscopy with standard surface analysis techniques.
- We apply TOF-DRS to detect rows of Cu vacancies in the $(3\sqrt{2}x\sqrt{2})R45^{o}$ Sn/Cu(001) surface.
- The formation of SAMs of BDMT on Cu(001) from the vapour phase is studied.